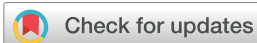


REVIEW



Cite this: *J. Mater. Chem. C*, 2018, **6**, 11878

Recent progress in flexible pressure sensor arrays: from design to applications

Jing Li,^{†ab} Rongrong Bao,^{†ab} Juan Tao,^{ab} Yiyao Peng^{ab} and Caofeng Pan^{id*ab}

Flexible pressure sensors that can maintain their pressure sensing ability with arbitrary deformation are of important significance in the fields of electronic skin, human-machine interfaces and medical diagnosis and treatment. To date, flexible pressure sensors have been studied extensively, and diverse transduction principles as well as different structural designs can be introduced to produce flexible pressure sensors that are capable of conformably covering an arbitrary surface. Moreover, high-performance flexible pressure sensors have been designed for different application needs. For example, high-resolution flexible pressure sensor arrays have been achieved based on piezoelectric nanowires (NWs); meanwhile crack-based pressure sensors with an extraordinarily simple structure have high sensitivity to tiny pressure, such as sound and physiological signals. For broader applications, endowing flexible pressure sensors with the sensing abilities of temperature, humidity and other stimuli are being developed to mimic the somatosensory system of human skin. In recent years, the development of novel flexible pressure sensors has been burgeoning with new sensors developed with self-powered, self-healing and biodegradable abilities. Here, we present comprehensive descriptions of the recent flexible pressure sensors, and then propose the potential prospects of flexible pressure sensors integrated with high sensitivity, high resolution, fast response, good stretchability and a wide detection range together, further enriching the multifunctions of flexible pressure sensors.

Received 15th June 2018,
Accepted 17th August 2018

DOI: 10.1039/c8tc02946f

rsc.li/materials-c

^a CAS Center for Excellence in Nanoscience, Beijing Institute of Nanoenergy and Nanosystems, Chinese Academy of Sciences, Beijing 100083, P. R. China.
E-mail: cfpan@binn.cas.cn

^b School of Nanoscience and Technology, University of Chinese Academy of Sciences, Beijing 100049, P. R. China

[†] These authors contributed equally to this work.

1 Introduction

Flexible pressure sensors can provide significant information about the specific demands inside the human body and in the processes where humans contact with their external environment. Conventional pressure sensors are typically made of stiff



Jing Li

Jing Li received her undergraduate degree in Materials Physics from the University of Science and Technology Beijing in 2016. She is currently a master's student with Prof. Caofeng Pan at Beijing Institute of Nanoenergy and Nanosystems, Chinese Academy of Sciences. Her current research interests focus on flexible tactile sensor arrays and their applications in electronic skin.



Rongrong Bao

Rongrong Bao received her BS degree from Tianjin University in 2007 and her PhD from the Technical Institute of Physics and Chemistry, Chinese Academy of Science, in 2012. She had been a postdoc fellow in the same institute. Now she has been an associate professor in the group of Prof. Caofeng Pan at Beijing Institute of Nanoenergy and Nanosystems, CAS, since 2016. Her main research interests focus on the fields of the production and characterization of organic-inorganic composite nano-devices and flexible pressure sensors.

materials and as such are mostly impracticable for flexible contacts or wearable devices. Hence, flexible pressure sensors compliant with arbitrarily curvilinear surfaces have been explored and are of great importance in the fields of human-machine interfaces, soft robotics, e-skin and medical diagnosis and treatment.^{1–9} However, in order to adapt these emerging applications realistically, flexible pressure sensors face the challenges of achieving high performance in the aspects of high sensitivity, high resolution, fast response, good stability and strong robustness.¹⁰ In addition, equipping flexible pressure sensors with multifunction to realize the feasibility of being applied in various complex environments is imperative for their wider application.

Lots of scientific research has been concentrated on the development of flexible pressure sensors. Above all, realizing the functionality of flexible pressure sensors is mainly based on two aspects: the transduction principles of pressure sensing and the methods to realize flexibility. Various transduction principles have been utilized to prepare flexible pressure sensors, broadly with exploration of flexible and functional materials.^{11–15} A large number of studies have also developed flexible pressure sensors by means of rational structure designs.^{16–18}

Furthermore, in order to satisfy the requirements of industrial production and practical applications, a lot of reports have focused on enhancing the performance of flexible pressure sensors. Among these, it is noteworthy that the piezoelectric and piezo-phototronic effects have been explored in NWs and introduced in pressure sensing, accomplishing a high resolution beyond the resolution of human skin,^{19–23} which has a profound meaning for developing electronic touchpads and soft robotics. Subsequently, in order to mimic the several sensory receptors of the human skin, flexible multifunctional pressure sensors are being explored with different sensing modules that are able to distinguish multi-stimuli from complicated surroundings.^{6,24–30} Moreover, while cracks are always regarded as damage in a device, introducing an extraordinarily simple crack-based structure into pressure sensing has drawn much attention for their ultrasensitive response to tiny deformations.^{31–33}

In recent years, novel flexible pressure sensors with self-powered, self-healing and biodegradable abilities are emerging and opening up a new research field. Since the discovery of nanogenerators by Wang's group in 2006, self-powered flexible pressure sensors have been seen as promising candidates in mobile electronics.^{34–41} Inspired by the tactile sensing and healable properties of human skin, flexible pressure sensors made of self-healing materials could guarantee long-term usage and economic efficiency.^{42–44} In addition, biodegradable pressure sensors have attracted much attention because of their advantages of being eco-friendly, biocompatible and having the potential to be applied in medical diagnostic and clinical therapeutic applications.^{3,5,45,46}

In this review, we focus on providing an introduction to the fundamental designs and improvements in the performance of flexible pressure sensors. In the next section, we present the primary transduction principles for pressure sensing and various strategies that can be used to achieve stretchability. In Section 3, we highlight the different flexible pressure sensors with good performance in terms of high resolution, multi-function and ultrahigh sensitivity, and then address novel



Juan Tao

Juan Tao received her undergraduate degree from China University of Geosciences (Beijing) in 2015. Currently, she is pursuing her PhD under the supervision of Prof. Caofeng Pan at Beijing Institute of Nanoenergy and Nanosystems, CAS. Her research is mainly focused on self-powered systems and flexible pressure sensor devices, and their applications in human-computer interaction interfaces.



Yiyao Peng

Yiyao Peng received her undergraduate degree from China University of Geosciences (Beijing) in 2015. She is currently pursuing her PhD under the supervision of Prof. Caofeng Pan at Beijing Institute of Nanoenergy and Nanosystems, CAS. Her research is mainly focused on photoelectric devices and the electronic applications of piezophototronics.



Caofeng Pan

Caofeng Pan received his BS degree (2005) and his PhD (2010) in Materials Science and Engineering from Tsinghua University, China. Then he joined the group of Professor Zhong Lin Wang at the Georgia Institute of Technology as a postdoctoral fellow. He is currently a professor and a group leader at Beijing Institute of Nanoenergy and Nanosystems, Chinese Academy of Sciences since 2013. His research interests mainly focus on the fields of piezotronics/piezophototronics for fabricating new electronic and optoelectronic devices. Details can be found at <http://www.piezotronic.cn/>.

flexible pressure sensors with self-powered, self-healing and biodegradable properties. Finally, we summarize the recent breakthroughs in flexible pressure sensors and outline the perspectives for flexible pressure sensors.

2. Fundamental designs of flexible pressure sensors

Lots of effort has been devoted to exploring efficient transduction principles for monitoring pressure stimuli from flexible contacts. Meanwhile, apart from achieving the pressure sensing ability, realizing flexibility and stretchability ensures the functionality of flexible pressure sensors when acting on curved surfaces. In this section, we introduce the fundamental design of flexible pressure sensors from the viewpoint of two aspects: pressure transduction principles and strategies to achieve stretchability.

2.1 Pressure transduction principles

Various transduction mechanisms involving piezoresistivity, capacitance and piezoelectricity have been explored to convert pressure stimuli into electrical signals. Based on the three transduction principles above, lots of works have been done to enhance the properties of flexible pressure sensors, with some flexible pressure sensors and their performance parameters summarized in Table 1. Besides, other transduction methods broadening the application of flexible pressure sensors have also been reported in recent years. These are all covered in this section below.

2.1.1 Piezoresistivity. The mechanism behind piezoresistive sensors is based on transducing pressure stimuli into a variation of resistance. Piezoresistive sensors have been widely studied due to their facile fabrication, simple structure, low cost and easy signal collection. The resistance change of piezoresistive sensors mainly comes from the contact resistance between two conductive modules under external pressure. Typically, a wearable pressure sensor is fabricated with the sandwich structure of an ultrathin Au NWs-impregnated tissue paper between a blank polydimethylsiloxane (PDMS) sheet and patterned interdigitated electrode arrays. When under external pressure, the contact resistance between the tissue paper and the interdigitated electrode decreases, which is due to there being more Au NWs in contact with the interdigitated electrode produced by the subtle compressive deformation (Fig. 1a).⁴⁷ Based on the contact resistance change under pressure and on the microstructured PDMS, the sensitivity of flexible pressure sensors could be enhanced utilizing a simple structure formed by assembling a flexible electrode with another reduced graphene oxide (rGO),^{48,49} graphene⁵⁰ or poly(3,4-ethylenedioxythiophene):poly(sodium-*p*-styrenesulfonate)/polyurethane dispersion (PEDOT:PSS/PUD)⁵¹ thin-film-based microstructured PDMS substrate face to face. Furthermore, combining active materials (*e.g.* carbon nanotubes (CNTs),⁵² Au films⁵³ or single-walled carbon nanotubes (SWNTs)²) with the microstructured PDMS substrates to form pressure sensors with interlocked structures can lead to enhanced sensitivity, a low detection limit and a fast response.

A number of other piezoresistive mechanisms utilized to transduce pressure stimuli have also been proposed. Inspired by the geometry of a spider's slit organ, a kind of crack-based ultrasensitive sensor was developed that was capable of sensing pressure by the connection and disconnection of the adjacent cracks under external pressure.³¹ Additionally, by employing a pencil-on-paper with a cantilever structure, the crack-based sensor succeeded in differentiating compressive and tensile stimuli.⁵⁴ Wearable pressure sensors have been developed based on carbon cottons fabricated from cotton through a pyrolysis process. The resistivity of such a sensor decreased under pressure due to the detachment and sliding of the carbon fibres in the PDMS matrix.⁵⁵ A textile pressure sensor fabricated of Nylon[®] fabric coated with rGO and arranged in a grid was developed and was shown to be sensitive to external pressure and able to sense the position of the force.⁵⁶ Furthermore, graphene foams/sponges/aerogels macrostructures have attracted attentions for producing flexible pressure sensors due to their resistivity changes under external pressure.^{57–59} Liao did important work developing freestanding graphene foams in a simple and facile method, which were sensitive enough for monitoring human blood pressure when attached to the wrist of a human.⁶⁰ Similarly, sponge-like structures composed of CNT and PDMS have also been introduced in pressure sensing.^{61,62} In particular, MXenes (Ti₃C₂), which are two-dimensional early transition metal carbides and carbonitrides, are sensitive to pressure due to their relatively wide interlayer distance. External pressure stimuli decrease the distance between two neighbouring interlayers in MXene, which consequently reduces the internal resistance.⁶³

2.1.2 Capacitance. Capacitive pressure sensors are mainly based on a parallel plate capacitor, and the capacitance is determined by the equation: $C = \epsilon_0 \epsilon_r A/d$, where ϵ_0 and ϵ_r are the dielectric constants of the vacuum and the dielectric layer, A represents the overlapping area and d is the distance between two electrodes. When applying pressure perpendicularly to the electrodes, d changes, leading to a variation in the capacitance, whereas A changes with shear force.¹⁸

By optimizing the dielectric layer with microstructures,^{12,64} embedding silver NWs into the dielectric layer⁶⁵ or dispersing nanoparticles on the surface of dielectric layer,⁶⁶ the sensitivity of the capacitive sensor can be enhanced remarkably, in which the former results from the reduced d and the latter two result from higher ϵ_r . Among these, endowing a dielectric layer with microstructures reduces the visco-elastic behaviour as well as the response and relaxation times extraordinarily. Other structure designs are also utilized to improve the performance of capacitive pressure sensors. Inspired by microhair architectures, Bao *et al.* introduced microhair interfacial structures to a capacitive sensor so as to enable contact with an irregular surface more conformally, and this showed a 12-fold enhancement in the signal-to-noise ratio.⁶⁷

Capacitive pressure sensors can realize high transparency and biocompatibility by replacing the electrodes with ionic conductors (Fig. 1b),^{8,68} which mostly possess long-term stability and stretchability. By utilizing ion-containing hydrogels as

Table 1 Summary of some flexible pressure sensors and their performance indicators

Transduction principles	Advantages/disadvantages	Key materials	Sensitivity	Detection range	Linearity	Response time	Cyclic stability	Ref.
Piezoresistivity	<ul style="list-style-type: none"> ✓ High sensitivity ✓ Wide detection range ✓ Low cost and simple structures ✓ Easy signal collection ✗ Hysteresis effect ✗ Low resolution 	<ul style="list-style-type: none"> Ultrathin gold nanowires with interdigitated electrodes Hollow-sphere microstructure with microstructured conducting polymer thin film Interlocked Mimosa-molded PDMS coated with Ti/Au 	<ul style="list-style-type: none"> 1.14 kPa⁻¹ 56.0–133.1 kPa⁻¹ ($P < 30$ Pa) < 0.4 kPa⁻¹ ($P > 1$ kPa) 50.17 kPa⁻¹ ($P < 70$ Pa) 1.38 kPa⁻¹ (200 Pa < $P < 1.5$ kPa) 	<ul style="list-style-type: none"> 13–50 000 Pa 1–100 kPa 10.4 Pa–1.5 kPa 	<ul style="list-style-type: none"> Linear Nonlinear Two consecutive linearity region 	<ul style="list-style-type: none"> 17 ms 50 ms 20 ms 	<ul style="list-style-type: none"> 50 000 cycles (0–2.5 kPa) 8000 cycles (0–5 kPa) 10 000 cycles (156 Pa) 	<ul style="list-style-type: none"> 47 16 53
Capacitance	<ul style="list-style-type: none"> ✓ High sensitivity ✓ High resolution ✓ Low power consumption ✓ Large-area fabrication and low cost ✗ Complex readout element 	<ul style="list-style-type: none"> OTFT with microstructured PDMS dielectric OTFT with suspended gate Dielectric interlayer filled with Ag NWs 	<ul style="list-style-type: none"> 8.4 kPa⁻¹ ($P < 8$ kPa) 0.38 kPa⁻¹ ($P > 30$ kPa) 192 kPa⁻¹ 5.54 kPa⁻¹ ($P < 30$ Pa) 0.88 kPa⁻¹ ($P > 30$ Pa) 	<ul style="list-style-type: none"> 0–60 kPa 100–5 kPa 0–60 Pa 	<ul style="list-style-type: none"> Two consecutive linearity region Linear Two consecutive linearity region 	<ul style="list-style-type: none"> 10 ms 10 ms Not known 	<ul style="list-style-type: none"> 15 000 cycles (0–3 kPa) 100 000 cycles (0–1 kPa) 200 cycles (bending radius of 2 mm) 	<ul style="list-style-type: none"> 72 73 65
Piezoelectricity	<ul style="list-style-type: none"> ✓ High sensitivity ✓ High resolution ✓ Low power consumption ✓ Fast response ✗ Poor stretchability 	<ul style="list-style-type: none"> P(VDF-TrFE) nanofibers 2D ZnO nanoplatelets based piezotronic transistor Piezotronic transistor based on ZnO twin nanoplatelet 	<ul style="list-style-type: none"> 1.1 V kPa⁻¹ 60.97–78.23 meV MPa⁻¹ 1448.08–1677.53 meV MPa⁻¹ 	<ul style="list-style-type: none"> 0.1–2 kPa 0–3.64 MPa 0–152.88 kPa 	<ul style="list-style-type: none"> Linear Approximately linear Approximately linear 	<ul style="list-style-type: none"> Not known 5 ms 5 ms 	<ul style="list-style-type: none"> 1000 cycles (curvature of 74 mm) 5 h (0–1.84 MPa) Not known 	<ul style="list-style-type: none"> 75 77 78

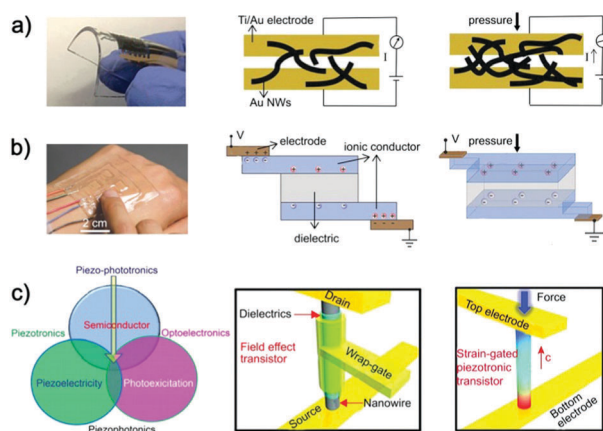


Fig. 1 Schematic diagram of the transduction principles, corresponding photographs of the devices and the piezotronics, piezophotonics, optoelectronics, and piezo-phototronics on the basis of the three-way coupling among the semiconductor, piezoelectricity and photoexcitation relying on the piezopotential created by the piezoelectric materials: (a) piezo-resistivity. Reproduced with permission.⁴⁷ Copyright 2014, Springer Nature; (b) capacitance. Reproduced with permission.⁸ Copyright 2014, Wiley-VCH; (c) piezoelectricity. Reproduced with permission.^{21,76} Copyright 2010, 2013, Elsevier Ltd, American Association for the Advancement of Science, respectively.

electrodes, the structure of a disc-shaped electrode and a loop electrode separated by a dielectric layer, Madden *et al.* developed a capacitive pressure sensor array that was capable of detecting the motion of a finger while stretching or bending.⁶⁹

Integrating a capacitive mechanism into a transistor active matrix can derive ultrasensitive flexible pressure sensors, resulting from the signal amplification of the transistor active matrix.⁷⁰ Introducing a transistor active matrix with microstructured rubber dielectric layers or an air dielectric layer together with suspended gate electrodes are the two main methods to improve the sensitivity and reduce the response time.^{12,71} Bao *et al.* developed an active pressure sensor array by integrating a microstructured PDMS dielectric into an organic thin film transistor (OTFT). The capacitance of the dielectric layer changes with the applied pressure, and could be amplified strongly when the device was operated in the subthreshold regime, which endowed the pressure sensor array with a high sensitivity of 8.4 kPa^{-1} and a fast response of 10 ms.⁷² Zhu *et al.* developed an organic thin-film transistor array using suspended gate electrodes and replaced the rubber dielectric layer with an air dielectric layer. The as-fabricated transistor array was able to overcome the elastic limitation of the rubber dielectric layer, and could be optimized to possess an ultrahigh sensitivity of 192 kPa^{-1} and a fast response time of less than 10 ms.⁷³

2.1.3 Piezoelectricity. The working mechanism of piezoelectric pressure sensors is that dipole moments in the anisotropic crystalline materials are generated under external pressure stimuli and produce a macroscopic potential in crystals.⁷⁴ Both piezoelectric polymers and inorganic materials are widely exploited for tactile sensing. As a conductive polymer with good flexibility, low impedance and a relatively high piezoelectric voltage coefficient, poly(vinylidene fluoride) (PVDF) and its

copolymers are widely used in the sensing of acceleration, vibration and orientation.⁷⁵ Profiting from low cost and the ability for large area fabrication, PVDF and its copolymers have been extensively developed, but are subject to a low piezoelectric strain constant (d_{33}) towards pressure sensing.

On the contrary, inorganic materials with a non-central symmetry mostly possess high d_{33} and are thus applied extensively in pressure sensing, such as ZnO, GaN, InN, ZnS and CdS.²¹ Wu *et al.* prepared addressable two-terminal transistor arrays based on vertical ZnO NWs and employed strain as a gate to modulate the electric signal, with the as-fabricated transistor arrays achieving high-resolution tactile sensing and a self-powered property (Fig. 1c).⁷⁶ Importantly, the resolution of NW-based piezoelectric pressure sensor arrays generally depends on the size and distribution of the NWs or NW clusters, which endow piezoelectric pressure sensor arrays with the possibility for achieving high resolution. Recently, two-dimensional (2D) materials, such as ZnO^{77,78} and MoS₂,⁷⁹ have also been discovered to possess a piezoelectric effect and are promising candidates for piezoelectric pressure sensors. Liu *et al.* developed a 2D piezotronic transistor array based on assembling ZnO nanoplatelets into an ordered nanoplatelet array, with the transistor array deriving a high pressure/strain sensitivity of $60.97\text{--}78.23 \text{ meV MPa}^{-1}$ and a high resolution of 12 700 dpi.⁷⁷

2.1.4 Other transduction methods. Except for the transduction mechanisms mentioned above, other transduction principles have also been utilized to sense pressure. A resonant pressure sensor, with the structure of sandwiching a deformable dielectric layer between two inductive spirals was capable of detecting pressure, attributed to the resonant frequency shift under pressure.⁷ This kind of flexible pressure sensor initiated the wireless monitoring of the health index of humans for medical diagnosis and bioresearch. The optical pressure sensor employing polymer waveguides was applied on curvilinear interfaces.^{80,81} An optical pressure sensor was developed comprising PDMS waveguide, polymer organic light-emitting diodes (OLEDs) and a polymer organic photodiode. When external pressure stimuli were applied, the PDMS thickness was reduced as well as the light, which was detected by the photodiode due to the less modes supported by the waveguide.⁸⁰ Lately, triboelectric pressure sensors based on the coupling of contact electrification and electrostatic induction have drawn plentiful attention, and these can generate an electrical signal as a response to external stimulation without the need for a power supply.³⁴

2.2 Strategies to achieve stretchability

Equipping pressure sensors with flexibility and stretchability expands their application on rugged surfaces, which is necessary in the field of artificial intelligence and to address the practical needs of human-machine interaction. Flexible pressure sensors can be realized through reducing the thickness of the substrate or by employing flexible structures. For example, hollow-sphere microstructure and fractured conductive sponge have been used to fabricate flexible pressure sensors with high sensitivity.^{16,17} Compared with flexibility, stretchability is much harder to

achieve, and makes the pressure sensors deform continuously with the objects without damage and retaining the pressure sensing ability. Up to now, plenty of materials and structures have been exploited to realize stretchability. The two main approaches to achieve stretchability are utilizing the intrinsic stretchable materials and designing proper structure to acquire stretchability, respectively.

2.2.1 Intrinsic stretchability. Intrinsic stretchability of pressure sensors is achieved mostly through embedding active materials into the polymers with a high elastic modulus. By filling the surface layer of PDMS with SWCNTs and utilizing a perfluoro monolayer between the PDMS and SWCNTs, as-fabricated capacitive pressure sensors were able to withstand strains of up to 300%.⁸² However, embedding active materials into the polymers always results in changes of the mechanical compliance of the elastic polymers. Park and coworkers developed highly conformable and stretchable electrocardiogram (ECG) sensors by embedding Ag NWs into adhesive PDMS. The adhesive PDMS was achieved through adding a nonionic surfactant of Triton X into PDMS, which greatly improved the mechanical properties of the PDMS.⁸³ Shepherd *et al.* manufactured a hyperelastic light-emitting capacitor through utilizing an ionic hydrogel as the electrode and composites of doped ZnS phosphors embedded into a dielectric matrix of ecoflex as the dielectric layer, whereby the as-fabricated capacitor could sustain stretches of up to 480%.⁸⁴ Similarly, a highly stretchable, transparent capacitive ionic skin has been explored based on sandwiching a dielectric between two ionic conductors.⁸ Moreover, a capacitive sensor array was produced with grooves containing an ionically conductive interconnect, which could be clamped and stretched by 10%.⁶⁹ A composite film was prepared by dispersing SWNTs in a vinylidene fluoride-hexafluoropropylene copolymer matrix, whereafter a rubber-like active matrix was developed by integrating an elastic conductor with printed organic transistors, which could be uniaxially and biaxially stretched by 70% without mechanical or electrical damage.⁸⁵ Intrinsic stretchable pressure sensors mostly exhibit excellent stability, which is extremely important for their long-term application.

2.2.2 Structure-derived stretchability. Reasonable structure design can transform conventional fragile materials into stretchable components. Typically, a simple structure to achieve stretchability can be achieved by adhering conductive materials to stretchable polymer materials. For example, PDMS coated with SWNT⁵¹ and PEDOT:PSS⁸⁶ has served as an electrode for stretchable pressure sensors. In addition, a pressure sensor was obtained with a spring-like structure by spray-coating CNTs on a PDMS substrate, followed with it being stretched, and it could accommodate a strain of up to 150%.⁸⁷ Pan *et al.* took advantage of a stretchable serpentine-shaped electrode and fabricated a capacitive multifunctional sensor array that could be stretched by up to 70%.¹⁸ A three dimensional (3D) printing method has also been introduced in manufacturing a serpentine electrodes-based highly sensitive capillary pressure sensor, which exhibited great stretchability.⁸⁸ A pressure sensor array could maintain its performance under

biaxial stretching by 15%⁸⁹ with optimized PDMS micropillars incorporated for achieving stretchability.

3. Exploration of high-performance flexible pressure sensor arrays

With the development of social civilization and the economy, flexible pressure sensors with high-performance, such as high sensitivity, high resolution, fast response and great flexibility, are of significant importance for broad applications and have thus been researched extensively. Furthermore, to mimic the functionality of human skin, endowing the pressure sensor with multifunctions is imperative for smart prosthesis and humanoid robotics. Besides, novel flexible pressure sensors with self-powered, self-healing and biodegradable neoteric properties broaden the application field of mobile electronics, surgical medicine and artificial prosthetics. The recent research is highlighted briefly in this section.

3.1 High-resolution flexible pressure sensor arrays based on piezotronic/piezo-phototronic effect

Flexible pressure sensors present great application prospects in human-machine interfaces, touchpad technology, personalized signatures and bio-imaging, which require the characteristics of high resolution, high sensitivity and fast response. However, the resolution of a resistive and capacitive pressure array is mostly in the order of millimetres. Fortunately, miniaturizing the flexible pressure sensors has been achieved by utilizing the wurtzite structure of micron, nanomaterials such as ZnO, GaN and CdS NWs to produce piezotronic pressure sensor arrays. For the sake of visual pressure sensing, the piezo-phototronic effect, defined as the coupling effect of piezoelectricity, photonic excitation and semiconductor transport, is introduced to sensing pressure through tuning and controlling the electro-optical processes by a strain-induced piezopotential,²¹ which is capable of converting pressure into an optical signal and mapping the spatial pressure distribution.

For the purpose of achieving high-resolution pressure mapping, our group developed a pressure sensor array based on a piezoelectric NW LED, which had an unprecedented spatial resolution of 2.7 μm (equivalent to a pixel density of 6350 dpi) (Fig. 2). A single pixel of our light-emitting diode consisted of a single n-ZnO NW on a p-GaN substrate and electrodes, while the emission intensity was controlled by the local pressure resulting from the piezo-phototronic effect. Furthermore, by introducing parallel detection technology, pressure distribution maps could be created with a time resolution of 90 ms.²³ Afterwards, taking advantage of an indium tin oxide (ITO)/PET flexible substrate to replace the GaN/sapphire hard substrate, we demonstrated a flexible organic/inorganic hybridized LED array, which contained a PEDOT:PSS layer and a patterned n-type ZnO NWs array. When under external pressure, resulting from the non-central symmetric structure, a piezo-potential was created in the inner-crystal by the deviation of the centre of the cations and anions. The piezopotential tuned the

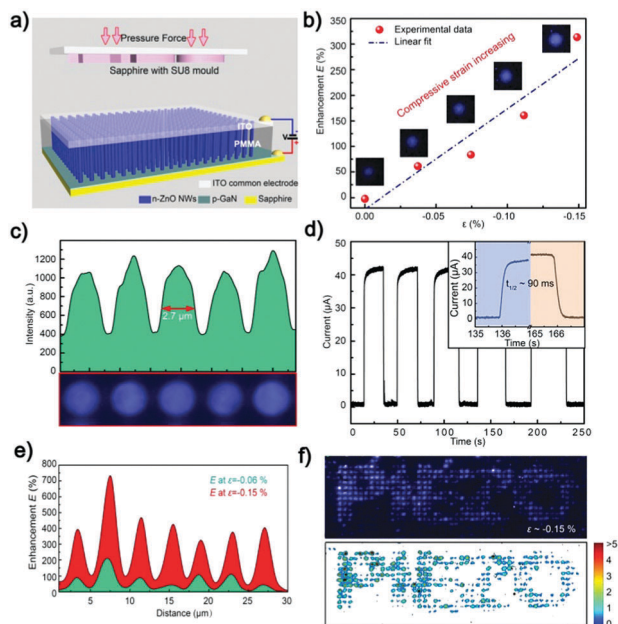


Fig. 2 High-resolution n-ZnO NW/p-GaN LED array for mapping the spatial distribution of pressure based on the piezo-phototronic effect. (a) Principle scheme of experimental approaches for pressure mapping. (b) The change of enhancement factor of a pixel in response to an external compressive strain and the corresponding emitting light images. (c) The resolution of the LED array was measured as 2.7 μm . (d) The response and recovery times of the LED were 90 ms. (e) The enhancement factor E of 7 pixels under strains of -0.06% and -0.15% . (f) High-resolution pressure mapping of the word 'PIEZO'. Reproduced with permission.²³ Copyright 2013, Springer Nature.

energy band in the ZnO side and dramatically increased the recombination rate of charge carriers in the ZnO NWs, which in turn yielded an increase in the light-emission intensity. By reading the illumination intensities of the array parallelly, the pressure distribution of letters "BINN" was obtained with a resolution of 7 μm (Fig. 3). Specifically, adjusting the growth conditions of the ZnO NW array could modulate the detection range of pressure between 40 and 100 MPa.¹⁹ Lately, based on the piezo-phototronic effect, a flexible CdS nanorods/PEDOT:PSS LED array on an Au/Cr/kapton flexible substrate was also investigated to map the pressure distribution and showed an enhanced resolution of 1.5 μm (Fig. 4).²²

ZnO NWs grown by the low-temperature hydrothermal approach often result in defect emission, which in turn brings about an uncontrollable colour and poor efficiency of emission. In order to reduce the effects mentioned above, our group developed a patterned ZnO NWs-based OLED array on a flexible ITO/PET substrate, in which the patterned ZnO NWs served as the unique stress response layer based on the piezotronic effect, while the properties of light emission relied on the organic layer exclusively (Fig. 5a). When pressure was applied on the device, the piezopotential reduced the Schottky barrier at the interface between the electrode and the semiconductor, increasing the current in the piezotronics transistors as well as the light-emission intensity of the OLED. The enhancement factor E , defined as the ratio of the luminous intensity under

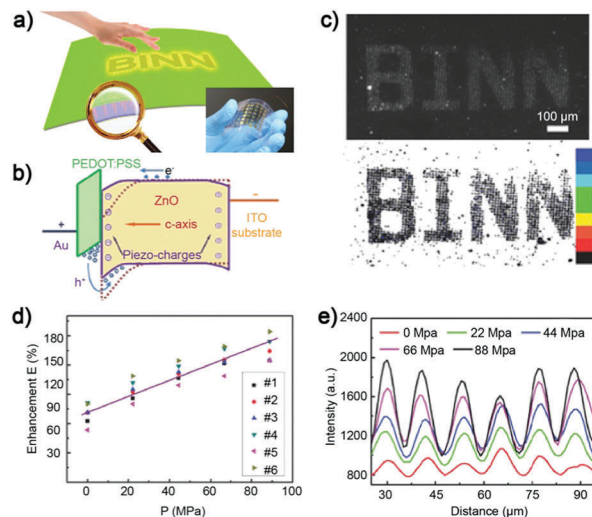


Fig. 3 Flexible ZnO NW/p-polymer LED array for pressure mapping based on the piezo-phototronic effect. (a) Schematic and photograph of the flexible LED array. (b) Schematic band diagram of a pixel under compressive strain. (c) High-resolution pressure distribution of the word 'BINN'. (d) The variation of enhancement factor of LEDs under different applied pressures. (e) The response to different external pressures. Reproduced with permission.¹⁹ Copyright 2015, Wiley-VCH.

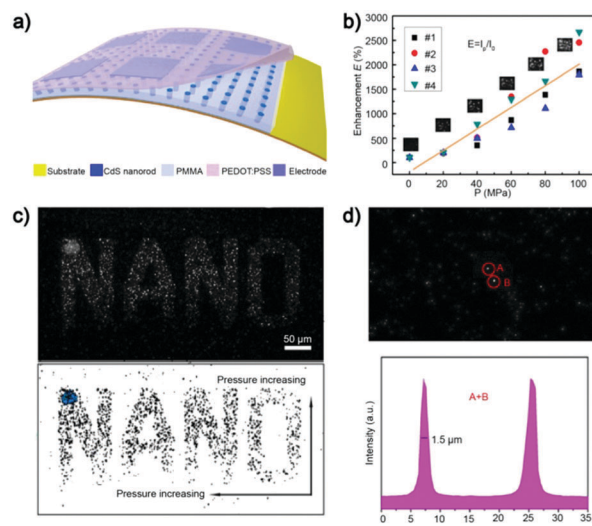


Fig. 4 Enhanced resolution derived from a flexible CdS nanorods/organic hybrid LED array based on the piezo-phototronic effect. (a) The schematic illustration of the device structure. (b) Enhancement factor of several LEDs in response to applied compressive pressures. (c) The pressure mapping of the pattern 'NANO'. (d) The resolution of the LED array was 1.5 μm . Reproduced with permission.²² Copyright 2016, Royal Society of Chemistry.

compression and the initial condition, was enhanced with the increase of the external compressive pressures (Fig. 5b).²⁰ By making use of different organic phosphorescent materials in the organic layer, the light-emission colour of the OLED could be adjusted to satisfy different application requirements (Fig. 5c).

Except for the utilization of piezoelectronic NWs, we also employed ZnS:Mn particles (ZMPs) prepared *via* a vacuum solid-state reaction to fabricate a wafer-scale, flexible pressure

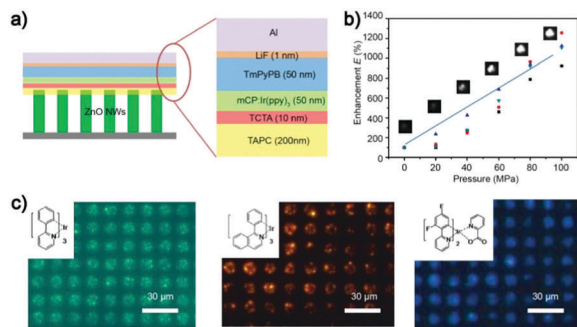


Fig. 5 Flexible ZnO NW/OLED array used for pressure mapping based on the piezotronic effect. (a) Schematic of the device structure. (b) Enhancement factor of the light-emission intensity of LEDs under diverse applied pressures. (c) Micrographs of the flexible devices with different colours. Reproduced with permission.²⁰ Copyright 2017, American Chemical Society.

sensor matrix based on the piezo-photonic effect (Fig. 6a). In this system, the potential produced by the piezo-charges under pressure surpasses the valence bands of ZnS and promotes non-radioactive recombination, which provides the energy for the excitation of Mn^{2+} ions, and yellow visible light is generated due to the de-excitation of Mn^{2+} ions (Fig. 6b). The integral intensity increases linearly with the increase in the external applied pressures in the working range of 10–50 MPa with a rapid response time of less than 10 ms (Fig. 6d). By utilizing the image acquisition unit and processing the optical signals, both a single-point dynamic pressure recording and a 2D planar pressures mapping could be achieved, which could record and distinguish the manuscript signatures as well as the signing customs of the signees (Fig. 6e). Large-scale ZMPs:photoresist arrays were fabricated through a UV photolithography technique with a spatial resolution of less than 100 μm (254 dpi), and the resolution could be further improved through other micropatterning technology.⁹⁰ On this basis, for the sake of controlling the doping amount accurately, a solid-state reaction under atmospheric pressure with the assistance of oxygen was

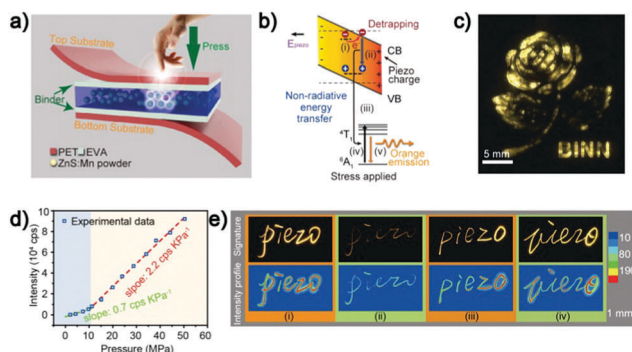


Fig. 6 Flexible pressure sensor matrix based on the piezo-phototronic effect. (a) Schematic diagram of the device structure. (b) Band diagram of the piezo-phototronic effect of ZMPs. (c) Visualization of the 2D planar pressure distributions of a stamp. (d) Integral intensity over 525–685 nm in response to different pressures. (e) Signing habits of four signees recorded by the flexible pressure sensor matrix. Reproduced with permission.⁹⁰ Copyright 2015, Wiley-VCH.

utilized to produce the ZMPs, and a flexible pressure sensor with a remarkable sensitivity of 0.032 MPa^{-1} was obtained.⁹¹ The flexible pressure sensors based on the piezotronic/piezo-phototronic effect are promising candidates for future high-performance pressure sensor arrays with high resolution and a fast response.

3.2 Endowing flexible pressure sensor arrays with multifunction

As for the application in e-skin, robotics and human-machine interfaces, pressure sensing together with temperature, humidity and other stimuli sensing are of great necessity. Decoupling the signal analysis and integrating multifunctional properties into one sensor array are the main challenges for multifunctional pressure sensors.

Based on an interlocking structure, a strain-gauge sensor was developed on a PDMS substrate with high-aspect-ratio polyurethane (PU)-based nanofibres coated with Pt. The strain-gauge sensor was capable of differentiating the stimuli of pressure, shear and torsion by decoupling the gauge factor (GF) of the acquired signal.²⁴ By integrating a piezo-pyroelectric nanocomposite gate dielectric and piezo-thermo-resistive organic semiconductor channel into an organic field effect transistor (OFET), a bimodal sensor array was fabricated to sense pressure and temperature through decoupling the signal from a single FET platform.²⁵ The main issue of the multifunctional sensor above was the signal interference during the process of the decoupling analysis. In order to achieve dynamic pressure detection as well as multifunction without the decoupling analysis, our group developed a parallel plate capacitor array by sandwiching an ecoflex silicone elastomer between Ag top and bottom electrodes with a serpentine-shaped structure. The as-fabricated pressure sensor array was capable of dynamically detecting the real-time spatial distributions of contact, pressure and strain, possessing a detection limit of 6 Pa stretched up to 70% (Fig. 7a).¹⁸ In addition, for mimicking the human skin in sensing pressure and temperature, Zhu *et al.* developed a temperature–pressure dual-parameter sensor array with a microstructured porous PU immersed in thermoelectric PEDOT:PSS, while the variation of contact resistance was used for sensing pressure and the output voltage was used for

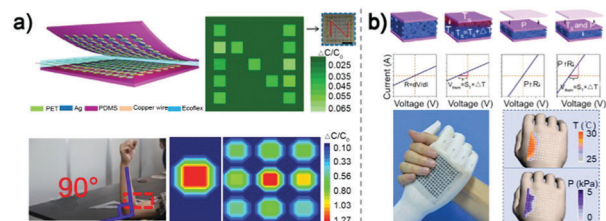


Fig. 7 Endowing a flexible pressure sensor array with multi-force and temperature sensing abilities. (a) Flexible, stretchable and wearable capacitive sensor array for sensing spatial contact, pressure and strain distributions. Reproduced with permission.¹⁸ Copyright 2015, Wiley-VCH. (b) Temperature–pressure dual-parameter sensor array based on piezo-resistivity and thermoelectricity. Reproduced with permission.²⁶ Copyright 2015, Springer Nature.

sensing temperature. The dual-parameter sensor array was installed on a prosthetic and was capable of spatially monitoring the temperature and pressure distribution of the prosthetic without the decoupling analysis when the prosthetic hand was used in arm-wrestling with an adult woman (Fig. 7b).²⁶ Furthermore, a gas-permeable and stretchable electrode with a conductive nanomesh structure was fabricated through electrospinning and depositing, and could then be directly adhered to human skin without inflammation. By integrating a flexible and thin polymeric temperature sensor with a positive temperature coefficient as well as a pressure-sensitive rubber, the on-skin sensors were able to detect pressure and temperature simultaneously.⁹²

For the application of flexible pressure sensors in e-skin, in addition to pressure and temperature sensing,^{27,93} endowing the pressure sensor with additional sensing abilities in one sensor array is required. Kim *et al.* developed a stretchable prosthetic skin with a stack layout of multifunctional sensors consisting of strain, pressure, temperature and humidity together with an electro-resistive heater for regulating body temperature. The ultrathin layout and stretchable electrodes design gave the prosthetic skin durability, mechanical stability and high sensitivity to multi-stimuli from surroundings.⁶ Inspired by the complex somatosensory system of human skin, a stretchable and conformable matrix network (SCMN) based on meandering interconnects was explored with the ability to sense temperature, in-plane strain, relative humidity, ultraviolet light, magnetic field, pressure and proximity (Fig. 8b). In particular, both distributed and stacked layouts of the sensor array could be achieved, while a potentially high density of the mechanoreceptor could be gained with stacked layouts. The sensor array could still maintain its sensing abilities when

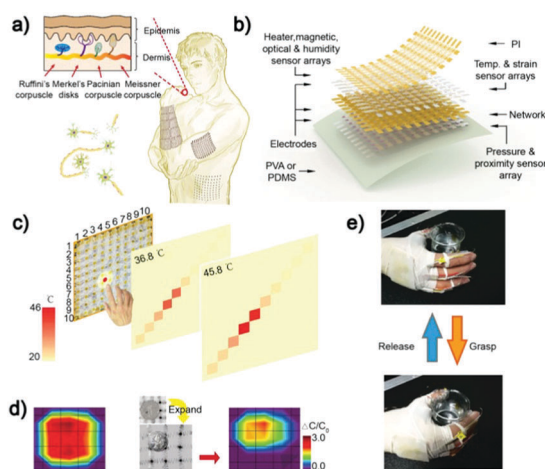


Fig. 8 Human-skin-inspired highly SCMN with the ability to sense temperature, in-plane strain, humidity, light, magnetic field, pressure and proximity. (a) Schematic illustration of SCMNs and an expanded network conformable to the surface of human skin; (b) schematic layout of an SCMN. (c) Spatial temperature distribution. (d) Pressure mapping of a coin before and after the 300% expansion of an SCMN. (e) Photographs of the intelligent prosthetic hand able to grasp and release cups filled with water. Reproduced with permission.¹ Copyright 2018, Springer Nature.

expanded to large area (Fig. 8d).¹ A personalized intelligent prosthetic hand was put up for monitoring the pressure distribution as well as for measuring the temperature when grasping objects concurrently when the intelligent prosthetic hand grasped and then released cups filled with water (Fig. 8). The development of sensor arrays integrating multifunctional properties opens up a new research field for their application in more complex circumstances.

3.3 Ultrasensitive crack-based flexible pressure sensor arrays for detecting tiny pressure

The tiny and ultralow-pressure sensing demands mainly comprise sound pressure, human motions and physiological signals of the human body,¹⁰ which always brings about subtle deformations and can hardly be detected by conventional flexible pressure sensors. Recently, crack-based flexible pressure sensors exhibited ultrahigh sensitivity to deformations coming from tiny pressure, vibration and strain. For characterizing the sensitivity, GF is used for the criterion and is defined as $GF = (R/R_0)/\epsilon$, where R/R_0 represents the relative resistance change under an external pressure and ϵ represents the strain. Inspired by the crack-shaped slit organs of spiders for sensing exceedingly subtle stress, Kang *et al.* developed an ultrasensitive multifunctional pressure sensor array for detecting tiny pressure, vibration and strain. The sensor array possessed a simple structure from depositing a thin Pt layer on a substrate of polyurethane acrylate (PUA), while the cracks were generated in a controlled manner in aspects of crack density and direction by mechanically bending the sensor to various radii of curvature. Benefitting from the disconnection–reconnection process of the crack junctions, the sensor was able to detect a pressure of 5 Pa, a vibration of frequency 200 Hz with an amplitude of 14 mm and possessed a GF of over 2000 in the strain range of 0–2%, which could be used for precisely monitoring the normal heart rate as well as after exercising.⁹⁴ Yang *et al.*³³ and Park *et al.*³² further optimized the sensitivity of crack-based sensors by modulating the process of pre-stretching and the crack depth, respectively. Next, our group focused on employing the crack-based sensor for applications in detecting the tiny strain of non-joint areas and recognizing anti-interference voices. The sensor was fabricated by depositing a Ti/Au layer on a PDMS substrate followed with a pre-stretching process for generating cracks and a release process for the formation of overlap of the cracks. When under small deformations, the resistance increases with the decrease in the overlap area between the neighbour cracks. Upon relatively large deformations, the neighbour cracks no longer contact with each other and the resistance depends on the tunnel effect. The as-fabricated sensor derived a high GF of approximately 5000 in the strain range of 0–1%, and could detect tiny pressure, such as normal breathing and deep breathing as well as distinguishing voice signals from the noise (Fig. 9a).⁹⁵ Combining the crack-based sensor and a cantilever structure, an electronic whiskers array was prepared using a pencil-on-paper method inspired by the mammalian vibrissa. The electronic whiskers array showed great performance for mapping the 3D spatial distribution of an object

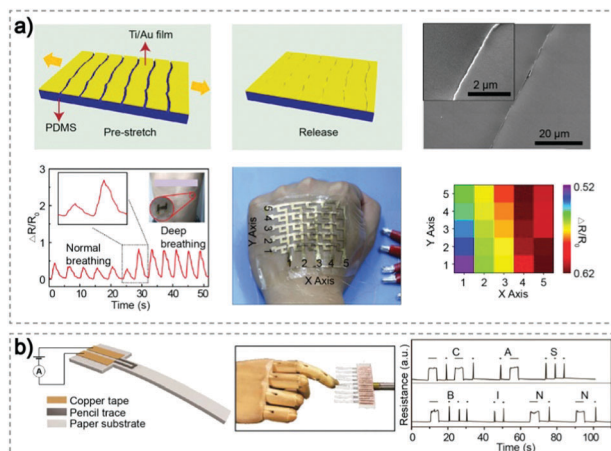


Fig. 9 Ultrasensitive crack-based pressure sensors for detecting tiny pressures. (a) Crack-based sensor for detecting the tiny strain of non-joint areas and recognizing anti-interference voices. Reproduced with permission.⁹⁵ Copyright 2017, Elsevier Ltd. (b) Mammalian vibrissa-inspired electronic whiskers array used for a human-machine interface and Morse code communication. Reproduced with permission.⁹⁶ Copyright 2016, Wiley-VCH.

together with its localization, orientation, shape and size (Fig. 9b).⁹⁶ Utilizing the Marangoni effect at the liquid/air interface, Zhu *et al.* developed self-assembled large-area ultrathin graphene films with a thickness of 2.5–5.0 nm. Based on the tunnelling effect of the overlapping area of graphene flakes, the as-fabricated strain sensor was highly sensitive to small deformation.⁹⁷ The ultrasensitive properties and high GF give crack-based sensor arrays enormous potential in health monitoring, human-machine interfaces and voice recognition.

3.4 Self-powered flexible pressure sensor arrays

Recently, self-powered pressure sensors have been studied in order to reduce the power consumption and broaden the applications in mobile electronic devices. The piezoelectric and triboelectric effects are the two main methods in self-powered systems. Self-powered pressure sensors based on the triboelectric effect have grown fast due to their simple, low-cost scalable fabrication process and ability to integrate with other processing technologies.

The fundamental principle of the triboelectric effect is the coupling of contact electrification and the electrostatic induction. Four basic modes have been explored for fabricating triboelectric nanogenerators (TEBG): the vertical contact-separation mode, lateral sliding mode, single-electrode mode and freestanding triboelectric-layer mode.³⁴ Among these, the vertical contact-separation mode and single-electrode mode are the most widely used for pressure sensing. The first flexible nanogenerator based on the contact-separation mode for pressure sensing was demonstrated by using transparent polymer materials and optimized using a micro-patterned surface, which was capable of sensing the pressure of a water droplet and a falling feather.⁹⁸ Inspired by the gradient stiffness between the epidermis and soft skin together with the interlocked structures of human skin, Ko *et al.* developed highly sensitive triboelectric sensors for detecting the important signs

and voices based on a contact-separation mode.⁹⁹ Zhu *et al.* developed ultrasensitive flexible tactile sensors based on the single-electrode mode with the structure of a sandwiched PET layer with two transparent ITO electrodes, in which a layer of fluorinated ethylene propylene (FEP) with vertically aligned polymer NWs acted as an electrification layer on the top and a nylon film served as a protection layer on the bottom. Benefitting from the modification of the electrification layer, the pressure sensors possessed a high sensitivity of $0.09\% \text{ Pa}^{-1}$ without an external power supply.¹⁰⁰ Based on the single-electrode mode as well, Pu *et al.* developed triboelectric nanogenerators mounted on an eyeglass arm for an electrooculogram-based human-machine interface, which could be utilized as a control signal for people.³⁵ Recently, by sandwiching TENG between two supercapacitors, Wang *et al.* developed a biomimetic pressure sensor that could detect both static and dynamic pressures. The voltage of the supercapacitor was used to detect the static pressure, while the outputs of the TENG were utilized to monitor the dynamic pressure. Meanwhile, the energy produced by the TENG could be stored in the supercapacitors efficiently.¹⁰¹

As for the pressure mapping, self-powered matrices of pressure sensors have been explored.^{102–104} Our group did a highlighted work for exploring a pressure-sensitive triboelectric sensor matrix with a resolution of 5 dpi and a high sensitivity of 0.06 kPa^{-1} , which could detect a single-point touch trajectory and map the multi-point pressure distribution in real time (Fig. 10a).³⁶ Next, by coupling the triboelectrification and electroluminescence, we reported a novel triboelectrification-induced electroluminescence effect of transducing human motions of even extremely weak stimuli into luminescence. The relative motion between two materials with different electronegativities results in tribocharges, which in turn change the ambient electric potential with an amplitude of hundreds of volts in milliseconds and excite the electroluminescence of the phosphor below. The as-fabricated self-powered pressure sensor possessed a high sensitivity of 0.03 kPa^{-1} in the low pressure range of less than 20 kPa and motions as low as 1 cm s^{-1} could be monitored. Benefitting from micro-nano

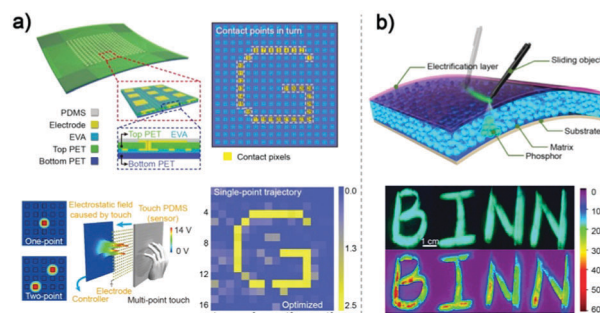


Fig. 10 Self-powered pressure sensor arrays based on the triboelectric effect. (a) Triboelectric sensor matrices (TESMs) for real-time tactile mapping. Reproduced with permission.³⁶ Copyright 2016, Wiley-VCH. (b) Visualized pressure sensing based on triboelectrification-induced electroluminescence. Reproduced with permission.¹⁰⁵ Copyright 2016, Wiley-VCH.

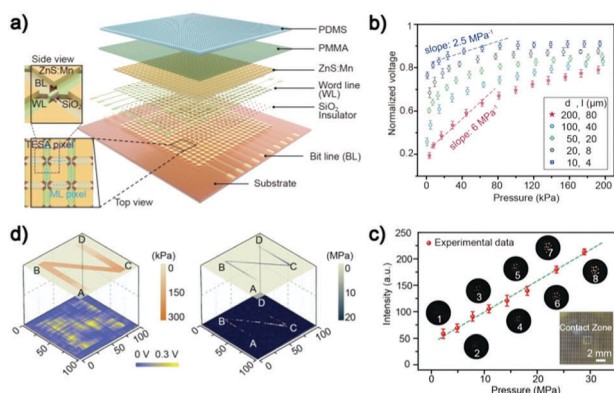


Fig. 11 Optical and electrical dual-mode full dynamic-range pressure sensor matrix for pressure distribution mapping. (a) Schematic of the device structure. (b) The normalized voltage in response to pressure. (c) The mechanoluminescent intensity under different applied pressures. (d) Electrical output voltage and optical signal of the pressure sensor matrix. Reproduced with permission.³⁸ Copyright 2017, Wiley-VCH.

fabrication technology and an image acquisition system, a high resolution was achieved by equipping the self-powered pressure sensor with a segmented structure, and the visual pressure distribution mapping of letters 'BINN' was derived (Fig. 10b).¹⁰⁵ After that, by combing an electroluminescent sensor matrix based on ZMPs and the single-electrode triboelectric nanogenerator matrix, a full dynamic-range pressure sensor matrix without an external power supply was fabricated with a high resolution of 100 dpi, which possessed high sensitivities of 6 and 0.037 MPa⁻¹ in the detection ranges of 0.6–200 kPa and 650 kPa to 30 MPa, respectively. The pressure sensor matrix could map the spatial distribution of both large and small pressures (Fig. 11).³⁸ Recently, Zhang *et al.* fabricated a self-powered flexible pressure sensor array with a high resolution of 127 × 127 dpi by assembling carbon fibres distributed vertically. Based on the single-electrode mode, the sensor array succeeded in tracking and mapping the movement of a tip.¹⁰⁶ Benefitting from the high sensitivity, fast response, long-term stability and low power consumption, flexible self-powered pressure sensor arrays can be applied in the fields of touchpad technology, human-machine interfacing and skin-like electronics.

3.5 Self-healing and biodegradable flexible pressure sensor arrays

Inspired by the advantages of human skin with the abilities of wound healing and metabolism, lots of efforts have been concentrated on self-healing and biodegradable materials and devices. Self-healing materials are a kind of novel material that can heal after being destroyed by an external force. Research into equipping pressure sensors with the ability of self-healing is booming currently for improving their working life and durability.¹⁰⁷ Usually, flexible pressure sensors are expected to work for a long time, whereas biodegradable electronics made of biodegradable materials are expected to be dissolves, resorbed or to physically vanish after working.⁴⁵ Biodegradable materials, such as semiconductors, dielectrics and metals, have been introduced in fabricating biodegradable pressure sensors,

which could then be applied to monitor intracranial pressure,⁵ orthopaedic rehabilitation³ and cardiovascular monitoring.⁴ For application in surgical medicine, biodegradable electronics can avoid second surgeries for device reception and can reduce the risk of infection. Biodegradable electronics are also environmentally friendly and are able to destruct after functioning, which means they can be used as data-secure hardware.

The first self-healing pressure sensor was developed by Bao and coworkers, which was manufactured with a supramolecular organic polymer to form a hydrogen bonding network embedded with nickel nanostructure microparticles. Plenty of weak hydrogen bonds in the composite materials break prior to the breakage of the covalent bonds when suffering damage, but the 'broken' hydrogen bonds have the ability to associate and dissociate at room temperature dynamically, which makes the composite materials self-healing. External pressure can change the space of nickel microparticles as well as their resistance simultaneously, so the composite materials achieve a piezo-resistive performance. A pressure sensor was developed by sandwiching the piezoresistive composite between layers of conductive composite, and was then mounted on the palm of a humanoid mannequin with electric circuits using LEDs for indicating the pressure. Tactile pressure could be detected through the resistance change, which in turn changed the intensity of the LEDs.¹⁰⁸ In order to improve the stretchability, Wang *et al.* developed a self-healing composite using a simple solution approach, in which polyaniline chains and polyacrylic acid served as the soft counterpart while phytic acid was used as a dopant to provide accessional physical crosslinking points. The as-fabricated composites could sustain a high stretchability of 500% approximately. A pressure sensor was fabricated by sandwiching a microstructured piezoresistive composite between two thin copper foils, and exhibited a high sensitivity of 37.6 kPa⁻¹ and 1.9 kPa⁻¹ in the range of 0–0.8 kPa and higher than 5 kPa, respectively.⁵⁰ Recently, the first dynamic covalent thermoset-based e-skin sensitive to tactile, temperature, flow and humidity was reported (Fig. 12a). By doping

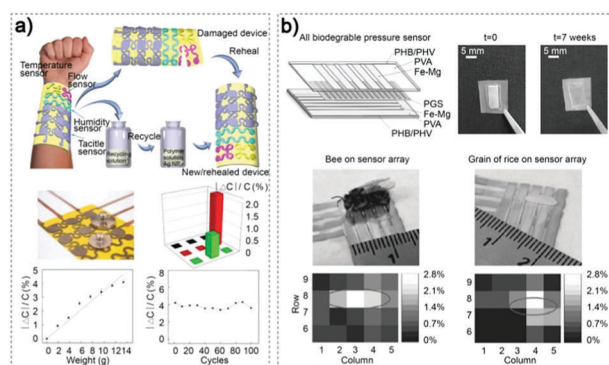


Fig. 12 Self-healing and biodegradable flexible pressure sensors. (a) A self-healing and malleable e-skin based on a dynamic covalent thermoset doped with silver nanoparticles. Reproduced with permission.⁴³ Copyright 2018, American Association for the Advancement of Science. (b) Flexible capacitive pressure sensor array made of biocompatible and biodegradable materials for pressure mapping. Reproduced with permission.⁴ Copyright 2015, Wiley-VCH.

polyimine with conductive silver nanoparticles, the composite possessed self-healing and malleable properties, which enabled the composite to maintain its mechanical and electric performance while simultaneously being conformable to sophisticated, irregular surfaces. In particular, the composite accorded environmental and economic benefits due to its recyclable and degradable properties. A pressure sensor array was explored by introducing a dielectric array into two conductive composite arrays on a polyimine substrate with serpentine structures to reduce the influence of strains. The pressure sensor array was able to detect the pressure distribution with a high sensitivity of 0.0067 kPa^{-1} and a detection limit between 0 and 14 g.⁴³

A biodegradable wireless RF pressure sensor was explored using zinc/iron bilayers and the polymers poly-L-lactide and polycaprolactone as the conductor, dielectric and structural materials, which derived a sensitivity of 39 kHz kPa^{-1} in the pressure range of 0–20 kPa in air and in the original saline.¹⁰⁹ To improve the sensitivity in the low-pressure range, a flexible capacitive pressure sensor array made of biodegradable materials was developed by laminating a poly(glycerol sebacate) (PGS) microstructured dielectric layer with Mg/Fe electrodes on the polyhydroxybutyrate/polyhydroxyvalerate (PHB/PHV) top and bottom substrates, and this pressure sensor array showed a fast response together with high sensitivity (Fig. 12b).⁴ The pressure sensor array was capable of detecting the pressure distribution of a bee, a grain of rice and a bipod object with a detection limit of 3 Pa, and could degrade to 85% of its original weight when immersed in a phosphate-buffered saline (PBS) solution at 37 °C after seven weeks. Later, a stretchable capacitive pressure and strain sensor was developed and used all biodegradable materials with a stack layout, while a pressure sensor was fabricated by sandwiching a microstructured PGS dielectric layer between two Mg electrodes evaporated onto a polylactic acid (PLLA) substrate, and the strain sensor was based on the capacitive change of two thin film with comb Mg electrodes sliding relatively to each other. The pressure sensitivities were $0.7 \pm 0.4 \text{ kPa}^{-1}$ and $0.13 \pm 0.03 \text{ kPa}^{-1}$ in the pressure range of less than 1 kPa and higher pressures ($5 < p < 10 \text{ kPa}$) with a detection limit of 12 Pa. After implanting the sensor on the back of rats, the sensor could maintain operational for more than 2 weeks and degraded slowly.³ The 2D material of monolayer MoS_2 was also used to prepare bioabsorbable sensors that were sensitive to pressure, temperature, strain and acceleration. The lifetime of the multi-functional sensor could be modulated by the grain size and the density of the monolayer MoS_2 grown by chemical vapour deposition, with these investigation results paving the way for introducing 2D materials into biodegradable electronics.⁴⁶

4. Conclusion and perspectives

In this review, we introduced the recent major progress in flexible pressure sensor arrays, covering their fundamental design to device application. Various transductions for pressure sensing and active materials together with structure designs for

achieving stretchability have improved the properties of flexible pressure sensors from many diverse aspects. High-resolution flexible pressure sensor arrays based on piezoelectric NWs that surpass the resolution of human skin are of great significance for flexible electronics. Equipping flexible pressure sensors with additional sensing capacities further broadens their applications for complicated tasks. In particular, ultrasensitive flexible pressure sensors were explored for detecting subtle deformations. Moreover, extending self-powered electronics to pressure sensing immensely lowers their power consumption, even without a power supply. Burgeoning self-healing and biodegradable materials are being embellished and introduced into flexible pressure sensors, which are making the flexible pressure sensors reusable, environmentally friendly and recyclable.

According to the application requirements of artificial intelligence, biomedicine and other fields, the future trend of sensor development is mainly in the following aspects. First, highly sensitive pressure sensors with an expanded detection range are necessary. Generally speaking, the best usage of a pressure sensor is within a certain range limited by the design of the sensor structure. Although sensors with specific detection ranges can be selected for different application needs, researchers are still trying to obtain a wide range of pressure sensors. There are sensors with a wide sensing range that combine more than two different sensing ranges. This design method will be one of the ways to solve this problem. Second, in order to meet the application requirements in the field of electronic skin, it is very important to develop pressure sensor arrays that can detect various physical quantities simultaneously. At present, most of the pressure sensor arrays with two or more physical quantities detection will not exclude the interaction between physical quantities. For instance, temperature has a great influence on all other physical quantities; however, measuring temperature is an indispensable ability of electronic skin. New active materials, structure designs and transduction principles can be looked forward to achieve this application requirement. Third, the self-powered sensor is a new trend in development in recent years. Pressure sensors based on the triboelectric effect provide a possible solution for realizing this function. This new type of pressure sensor in recent years still needs further research to design more functional sensors suitable for different applications. In addition to the above main trends of developments, high resolution and high sensitivity have been achieved by piezoelectric NWs-based pressure sensor arrays. Novel stretchable substrates for piezoelectric materials are expected to improve their stretchability and stability. Moreover, prosperous self-healing and biodegradable flexible pressure sensors are desired needing a deeper study into discovering more conductors and pressure-sensitive materials.

Conflicts of interest

There are no conflicts to declare.

Acknowledgements

The authors thank the support of National Key R & D Project from Minister of Science and Technology, China (2016YFA0202703), National Natural Science Foundation of China (no. 51622205, 61675027, 51432005, 61505010 and 51502018), Beijing City Committee of science and technology (Z171100002017019 and Z181100004418004), Beijing Natural Science Foundation (4181004, 4182080, 4184110 and 2184131) and the “Thousand Talents” program of China for pioneering researchers and innovative teams.

Notes and references

- Q. Hua, J. Sun, H. Liu, R. Bao, R. Yu, J. Zhai, C. Pan and Z. L. Wang, *Nat. Commun.*, 2018, **9**, 244.
- X. Wang, Y. Gu, Z. Xiong, Z. Cui and T. Zhang, *Adv. Mater.*, 2014, **26**, 1336–1342.
- C. M. Boutry, Y. Kaizawa, B. C. Schroeder, A. Chortos, A. Legrand, Z. Wang, J. Chang, P. Fox and Z. Bao, *Nat. Electron.*, 2018, **1**, 314–321.
- C. M. Boutry, A. Nguyen, Q. O. Lawal, A. Chortos, S. Rondeau-Gagne and Z. Bao, *Adv. Mater.*, 2015, **27**, 6954–6961.
- S. K. Kang, R. K. Murphy, S. W. Hwang, S. M. Lee, D. V. Harburg, N. A. Krueger, J. Shin, P. Gamble, H. Cheng, S. Yu, Z. Liu, J. G. McCall, M. Stephen, H. Ying, J. Kim, G. Park, R. C. Webb, C. H. Lee, S. Chung, D. S. Wie, A. D. Gujar, B. Vemulapalli, A. H. Kim, K. M. Lee, J. Cheng, Y. Huang, S. H. Lee, P. V. Braun, W. Z. Ray and J. A. Rogers, *Nature*, 2016, **530**, 71–76.
- J. Kim, M. Lee, H. J. Shim, R. Ghaffari, H. R. Cho, D. Son, Y. H. Jung, M. Soh, C. Choi, S. Jung, K. Chu, D. Jeon, S. T. Lee, J. H. Kim, S. H. Choi, T. Hyeon and D. H. Kim, *Nat. Commun.*, 2014, **5**, 5747.
- L. Y. Chen, B. C. Tee, A. L. Chortos, G. Schwartz, V. Tse, D. J. Lipomi, H. S. Wong, M. V. McConnell and Z. Bao, *Nat. Commun.*, 2014, **5**, 5028.
- J. Y. Sun, C. Keplinger, G. M. Whitesides and Z. Suo, *Adv. Mater.*, 2014, **26**, 7608–7614.
- Y. Kim, A. Chortos, W. Xu, Y. Liu, J. Y. Oh, D. Son, J. Kang, A. M. Foudeh, C. Zhu, Y. Lee, S. Niu, J. Liu, R. Pfattner, Z. Bao and T.-W. Lee, *Science*, 2018, **360**, 998–1003.
- Y. P. Zang, F. J. Zhang, C. A. Di and D. B. Zhu, *Mater. Horiz.*, 2015, **2**, 140–156.
- M. Kaltenbrunner, T. Sekitani, J. Reeder, T. Yokota, K. Kuribara, T. Tokuhara, M. Drack, R. Schwodiauer, I. Graz, S. Bauer-Gogonea, S. Bauer and T. Someya, *Nature*, 2013, **499**, 458–463.
- S. C. Mannsfeld, B. C. Tee, R. M. Stoltenberg, C. V. Chen, S. Barman, B. V. Muir, A. N. Sokolov, C. Reese and Z. Bao, *Nat. Mater.*, 2010, **9**, 859–864.
- T. Someya, T. Sekitani, S. Iba, Y. Kato, H. Kawaguchi and T. Sakurai, *Proc. Natl. Acad. Sci. U. S. A.*, 2004, **101**, 9966–9970.
- C. Wang, D. Hwang, Z. Yu, K. Takei, J. Park, T. Chen, B. Ma and A. Javey, *Nat. Mater.*, 2013, **12**, 899–904.
- Z. Chen, Z. Wang, X. Li, Y. Lin, N. Luo, M. Long, N. Zhao and J.-B. Xu, *ACS Nano*, 2017, **11**, 4507–4513.
- L. Pan, A. Chortos, G. Yu, Y. Wang, S. Isaacson, R. Allen, Y. Shi, R. Dauskardt and Z. Bao, *Nat. Commun.*, 2014, **5**, 3002.
- H. B. Yao, J. Ge, C. F. Wang, X. Wang, W. Hu, Z. J. Zheng, Y. Ni and S. H. Yu, *Adv. Mater.*, 2013, **25**, 6692–6698.
- Z. Xiaoli, H. Qilin, Y. Ruomeng, Z. Yan and P. Caofeng, *Adv. Electron. Mater.*, 2015, **1**, 1500142.
- R. R. Bao, C. F. Wang, L. Dong, R. M. Yu, K. Zhao, Z. L. Wang and C. F. Pan, *Adv. Funct. Mater.*, 2015, **25**, 2884–2891.
- R. R. Bao, C. F. Wang, Z. C. Peng, C. Ma, L. Dong and C. F. Pan, *ACS Photonics*, 2017, **4**, 1344–1349.
- Z. L. Wang, *Nano Today*, 2010, **5**, 540–552.
- R. Bao, C. Wang, L. Dong, C. Shen, K. Zhao and C. Pan, *Nanoscale*, 2016, **8**, 8078–8082.
- C. F. Pan, L. Dong, G. Zhu, S. M. Niu, R. M. Yu, Q. Yang, Y. Liu and Z. L. Wang, *Nat. Photonics*, 2013, **7**, 752–758.
- C. Pang, G. Y. Lee, T. I. Kim, S. M. Kim, H. N. Kim, S. H. Ahn and K. Y. Suh, *Nat. Mater.*, 2012, **11**, 795–801.
- N. T. Tien, S. Jeon, D. I. Kim, T. Q. Trung, M. Jang, B. U. Hwang, K. E. Byun, J. Bae, E. Lee, J. B. Tok, Z. Bao, N. E. Lee and J. J. Park, *Adv. Mater.*, 2014, **26**, 796–804.
- F. Zhang, Y. Zang, D. Huang, C.-A. Di and D. Zhu, *Nat. Commun.*, 2015, **6**, 8356.
- S. Han, J. Kim, S. M. Won, Y. Ma, D. Kang, Z. Xie, K. T. Lee, H. U. Chung, A. Banks, S. Min, S. Y. Heo, C. R. Davies, J. W. Lee, C. H. Lee, B. H. Kim, K. Li, Y. Zhou, C. Wei, X. Feng, Y. Huang and J. A. Rogers, *Sci. Transl. Med.*, 2018, **10**, DOI: 10.1126/scitranslmed.aan4950.
- M. Chunhong, S. Yuanqiang, H. Wutong, R. Ao, S. Rujie, X. Weihua and Z. Huaiwu, *Adv. Funct. Mater.*, 2018, **28**, 1707503.
- C. Yudong, L. Tie, G. Yang, L. Hui, W. Shuqi and Z. Ting, *Small*, 2018, **14**, 1703902.
- L. Zhiyuan, Q. Dianpeng, L. W. Ru, Y. Jiancan, X. Michele, C. Leonardo, L. Yaqing, Z. Bowen, J. Ying, C. Geng, M. Lorenzo, L. Bo and C. Xiaodong, *Adv. Mater.*, 2018, **30**, 1707285.
- D. Kang, P. V. Pikhitsa, Y. W. Choi, C. Lee, S. S. Shin, L. Piao, B. Park, K. Y. Suh, T. I. Kim and M. Choi, *Nature*, 2014, **516**, 222–226.
- B. Park, J. Kim, D. Kang, C. Jeong, K. S. Kim, J. U. Kim, P. J. Yoo and T. I. Kim, *Adv. Mater.*, 2016, **28**, 8130–8137.
- T. T. Yang, X. M. Li, X. Jiang, S. Y. Lin, J. C. Lao, J. D. Shi, Z. Zhen, Z. H. Li and H. W. Zhu, *Mater. Horiz.*, 2016, **3**, 248–255.
- S. H. Wang, L. Lin and Z. L. Wang, *Nano Energy*, 2015, **11**, 436–462.
- X. Pu, H. Guo, J. Chen, X. Wang, Y. Xi, C. Hu and Z. L. Wang, *Sci. Adv.*, 2017, **3**, e1700694.
- X. Wang, H. Zhang, L. Dong, X. Han, W. Du, J. Zhai, C. Pan and Z. L. Wang, *Adv. Mater.*, 2016, **28**, 2896–2903.
- Y. Zang, F. Zhang, D. Huang, X. Gao, C. A. Di and D. Zhu, *Nat. Commun.*, 2015, **6**, 6269.
- W. Xiandi, Q. Miaoling, C. Mengxiao, H. Xun, L. Xiaoyi, P. Caofeng and W. Z. Lin, *Adv. Mater.*, 2017, **29**, 1605817.

- 39 W. Li, D. Torres, R. Díaz, Z. Wang, C. Wu, C. Wang, Z. Lin Wang and N. Sepúlveda, *Nat. Commun.*, 2017, **8**, 15310.
- 40 B. Tianzhao, X. Tianxiao, Y. Zhiwei, L. Guoxu, F. Xianpeng, N. Jinhui, G. Tong, P. Yaokun, Z. Junqing, X. Fengben, Z. Chi and W. Z. Lin, *Adv. Mater.*, 2018, **30**, 1800066.
- 41 Y. Jie, H. Zhu, X. Cao, Y. Zhang, N. Wang, L. Zhang and Z. L. Wang, *ACS Nano*, 2016, **10**, 10366–10372.
- 42 T. P. Huynh and H. Haick, *Adv. Mater.*, 2016, **28**, 138–143.
- 43 Z. Zou, C. Zhu, Y. Li, X. Lei, W. Zhang and J. Xiao, *Sci. Adv.*, 2018, **4**, eaaq0508.
- 44 V. K. Thakur and M. R. Kessler, *Polymer*, 2015, **69**, 369–383.
- 45 R. Li, L. Wang, D. Kong and L. Yin, *Bioact. Mater.*, 2018, **3**, 322–333.
- 46 X. Chen, Y. J. Park, M. Kang, S. K. Kang, J. Koo, S. M. Shinde, J. Shin, S. Jeon, G. Park, Y. Yan, M. R. MacEwan, W. Z. Ray, K. M. Lee, J. A. Rogers and J. H. Ahn, *Nat. Commun.*, 2018, **9**, 1690.
- 47 S. Gong, W. Schwalb, Y. Wang, Y. Chen, Y. Tang, J. Si, B. Shirinzadeh and W. Cheng, *Nat. Commun.*, 2014, **5**, 3132.
- 48 B. Zhu, Z. Niu, H. Wang, W. R. Leow, H. Wang, Y. Li, L. Zheng, J. Wei, F. Huo and X. Chen, *Small*, 2014, **10**, 3625–3631.
- 49 S. Jidong, W. Liu, D. Zhaohe, Z. Lingyu, D. Mingde, L. Hongbian and F. Ying, *Small*, 2018, **14**, 1800819.
- 50 W. Tao, Z. Ying, L. Qingchang, C. Wen, W. Xinran, P. Lijia, X. Baoxing and X. Hangxun, *Adv. Funct. Mater.*, 2018, **28**, 1705551.
- 51 C. L. Choong, M. B. Shim, B. S. Lee, S. Jeon, D. S. Ko, T. H. Kang, J. Bae, S. H. Lee, K. E. Byun, J. Im, Y. J. Jeong, C. E. Park, J. J. Park and U. I. Chung, *Adv. Mater.*, 2014, **26**, 3451–3458.
- 52 J. Park, Y. Lee, J. Hong, M. Ha, Y. D. Jung, H. Lim, S. Y. Kim and H. Ko, *ACS Nano*, 2014, **8**, 4689–4697.
- 53 B. Su, S. Gong, Z. Ma, L. W. Yap and W. Cheng, *Small*, 2015, **11**, 1886–1891.
- 54 C. W. Lin, Z. Zhao, J. Kim and J. Huang, *Sci. Rep.*, 2014, **4**, 3812.
- 55 Y. Q. Li, Y. A. Samad and K. Liao, *J. Mater. Chem. A*, 2015, **3**, 2181–2187.
- 56 Y. A. Samad, K. Komatsu, D. Yamashita, Y. Q. Li, L. X. Zheng, S. M. Alhassan, Y. Nakano and K. Liao, *Sens. Actuators, B*, 2017, **240**, 1083–1090.
- 57 S. Y. Abdul, L. Yuanqing, S. Andreas, S. M. Alhassan and L. Kin, *Small*, 2015, **11**, 2380–2385.
- 58 Z. Chen, W. Ren, L. Gao, B. Liu, S. Pei and H.-M. Cheng, *Nat. Mater.*, 2011, **10**, 424.
- 59 G. Ge, Y. Cai, Q. Dong, Y. Zhang, J. Shao, W. Huang and X. Dong, *Nanoscale*, 2018, **10**, 10033–10040.
- 60 Y. A. Samad, Y. Li, S. M. Alhassan and K. Liao, *ACS Appl. Mater. Interfaces*, 2015, **7**, 9195–9202.
- 61 J.-W. Han, B. Kim, J. Li and M. Meyyappan, *Appl. Phys. Lett.*, 2013, 102.
- 62 X. Gui, A. Cao, J. Wei, H. Li, Y. Jia, Z. Li, L. Fan, K. Wang, H. Zhu and D. Wu, *ACS Nano*, 2010, **4**, 2320–2326.
- 63 Y. Ma, N. Liu, L. Li, X. Hu, Z. Zou, J. Wang, S. Luo and Y. Gao, *Nat. Commun.*, 2017, **8**, 1207.
- 64 B. C. K. Tee, A. Chortos, R. R. Dunn, G. Schwartz, E. Eason and Z. A. Bao, *Adv. Funct. Mater.*, 2014, **24**, 5427–5434.
- 65 J. Wang, J. Jiu, M. Nogi, T. Sugahara, S. Nagao, H. Koga, P. He and K. Suganuma, *Nanoscale*, 2015, **7**, 2926–2932.
- 66 K. Hyeohn, K. Gwangmook, K. Taehoon, L. Sangwoo, K. Donyoung, H. Min-Soo, C. Youngcheol, K. Shinill, L. Hyungsuk, P. Hong-Gyu and S. Wooyoung, *Small*, 2018, **14**, 1703432.
- 67 C. Pang, J. H. Koo, A. Nguyen, J. M. Caves, M. G. Kim, A. Chortos, K. Kim, P. J. Wang, J. B. Tok and Z. Bao, *Adv. Mater.*, 2015, **27**, 634–640.
- 68 B. Nie, R. Li, J. Cao, J. D. Brandt and T. Pan, *Adv. Mater.*, 2015, **27**, 6055–6062.
- 69 M. S. Sarwar, Y. Dobashi, C. Preston, J. K. Wyss, S. Mirabbasi and J. D. Madden, *Sci. Adv.*, 2017, **3**, e1602200.
- 70 S. Wang, J. Xu, W. Wang, G.-J. N. Wang, R. Rastak, F. Molina-Lopez, J. W. Chung, S. Niu, V. R. Feig, J. Lopez, T. Lei, S.-K. Kwon, Y. Kim, A. M. Foudeh, A. Ehrlich, A. Gasperini, Y. Yun, B. Murmann, J. B. H. Tok and Z. Bao, *Nature*, 2018, **555**, 83.
- 71 T. Sekitani, T. Yokota, U. Zschieschang, H. Klauk, S. Bauer, K. Takeuchi, M. Takamiya, T. Sakurai and T. Someya, *Science*, 2009, **326**, 1516–1519.
- 72 G. Schwartz, B. C. K. Tee, J. Mei, A. L. Appleton, D. H. Kim, H. Wang and Z. Bao, *Nat. Commun.*, 2013, **4**, 1859.
- 73 Y. Zang, F. Zhang, D. Huang, X. Gao, C.-A. Di and D. Zhu, *Nat. Commun.*, 2015, **6**, 6269.
- 74 Z. L. Wang, *Adv. Mater.*, 2012, **24**, 4632–4646.
- 75 L. Persano, C. Dagdeviren, Y. Su, Y. Zhang, S. Girardo, D. Pisignano, Y. Huang and J. A. Rogers, *Nat. Commun.*, 2013, **4**, 1633.
- 76 W. Wu, X. Wen and Z. L. Wang, *Science*, 2013, **340**, 952–957.
- 77 L. Shuhai, W. Longfei, F. Xiaolong, W. Zheng, X. Qi, B. Suo, Q. Yong and W. Z. Lin, *Adv. Mater.*, 2017, **29**, 1606346.
- 78 L. Wang, S. Liu, X. Feng, Q. Xu, S. Bai, L. Zhu, L. Chen, Y. Qin and Z. L. Wang, *ACS Nano*, 2017, **11**, 4859–4865.
- 79 W. Wu, L. Wang, Y. Li, F. Zhang, L. Lin, S. Niu, D. Chenet, X. Zhang, Y. Hao, T. F. Heinz, J. Hone and Z. L. Wang, *Nature*, 2014, **514**, 470–474.
- 80 M. Ramuz, B. C. Tee, J. B. Tok and Z. Bao, *Adv. Mater.*, 2012, **24**, 3223–3227.
- 81 S. Yun, S. Park, B. Park, Y. Kim, S. K. Park, S. Nam and K. U. Kyung, *Adv. Mater.*, 2014, **26**, 4474–4480.
- 82 X. L. Wang, T. J. Li, J. Adam and J. Yang, *J. Mater. Chem. A*, 2013, **1**, 3580–3586.
- 83 J.-H. Kim, S.-R. Kim, H.-J. Kil, Y.-C. Kim and J.-W. Park, *Nano Lett.*, 2018, **18**, 4531–4540.
- 84 C. Larson, B. Peele, S. Li, S. Robinson, M. Totaro, L. Beccai, B. Mazzolai and R. Shepherd, *Science*, 2016, **351**, 1071–1074.
- 85 T. Sekitani, Y. Noguchi, K. Hata, T. Fukushima, T. Aida and T. Someya, *Science*, 2008, **321**, 1468–1472.
- 86 H. H. Chou, A. Nguyen, A. Chortos, J. W. To, C. Lu, J. Mei, T. Kurosawa, W. G. Bae, J. B. Tok and Z. Bao, *Nat. Commun.*, 2015, **6**, 8011.

- 87 D. J. Lipomi, M. Vosgueritchian, B. C. Tee, S. L. Hellstrom, J. A. Lee, C. H. Fox and Z. Bao, *Nat. Nanotechnol.*, 2011, **6**, 788–792.
- 88 W. Liu and C. Yan, *Sensors*, 2018, **18**, 1001.
- 89 H. Park, Y. R. Jeong, J. Yun, S. Y. Hong, S. Jin, S. J. Lee, G. Zi and J. S. Ha, *ACS Nano*, 2015, **9**, 9974–9985.
- 90 X. Wang, H. Zhang, R. Yu, L. Dong, D. Peng, A. Zhang, Y. Zhang, H. Liu, C. Pan and Z. L. Wang, *Adv. Mater.*, 2015, **27**, 2324–2331.
- 91 X. D. Wang, R. Ling, Y. F. Zhang, M. L. Que, Y. Y. Peng and C. F. Pan, *Nano Res.*, 2018, **11**, 1967–1976.
- 92 A. Miyamoto, S. Lee, N. F. Cooray, S. Lee, M. Mori, N. Matsuhisa, H. Jin, L. Yoda, T. Yokota, A. Itoh, M. Sekino, H. Kawasaki, T. Ebihara, M. Amagai and T. Someya, *Nat. Nanotechnol.*, 2017, **12**, 907–913.
- 93 J. Park, M. Kim, Y. Lee, H. S. Lee and H. Ko, *Sci. Adv.*, 2015, **1**, e1500661.
- 94 D. Kang, P. V. Pikhitsa, Y. W. Choi, C. Lee, S. S. Shin, L. F. Piao, B. Park, K. Y. Suh, T. I. Kim and M. Choi, *Nature*, 2014, **516**, 222–226.
- 95 C. F. Wang, J. Zhao, C. Ma, J. L. Sun, L. Tian, X. Y. Li, F. T. Li, X. Han, C. T. Liu, C. Y. Shen, L. Dong, J. Yang and C. F. Pan, *Nano Energy*, 2017, **34**, 578–585.
- 96 H. Qilin, L. Haitao, Z. Jing, P. Dengfeng, Y. Xiaonian, G. Lin and P. Caofeng, *Adv. Electron. Mater.*, 2016, **2**, 1600093.
- 97 L. Xinming, Y. Tingting, Y. Yao, Z. Jia, L. Li, F. E. Alam, L. Xiao, W. Kunlin, C. Huanyu, L. Cheng-Te, F. Ying and Z. Hongwei, *Adv. Funct. Mater.*, 2016, **26**, 1322–1329.
- 98 F. R. Fan, L. Lin, G. Zhu, W. Wu, R. Zhang and Z. L. Wang, *Nano Lett.*, 2012, **12**, 3109–3114.
- 99 M. Ha, S. Lim, S. Cho, Y. Lee, S. Na, C. Baig and H. Ko, *ACS Nano*, 2018, **12**, 3964–3974.
- 100 G. Zhu, W. Q. Yang, T. Zhang, Q. Jing, J. Chen, Y. S. Zhou, P. Bai and Z. L. Wang, *Nano Lett.*, 2014, **14**, 3208–3213.
- 101 Z. Jingdian, Z. Meng, H. Jinrong, B. Jie, J. Yang, W. Magnus, C. Xia, W. Ning and W. Z. Lin, *Adv. Energy Mater.*, 2018, **8**, 1702671.
- 102 Y. Yang, H. Zhang, Z. H. Lin, Y. S. Zhou, Q. Jing, Y. Su, J. Yang, J. Chen, C. Hu and Z. L. Wang, *ACS Nano*, 2013, **7**, 9213–9222.
- 103 L. Lin, Y. Xie, S. Wang, W. Wu, S. Niu, X. Wen and Z. L. Wang, *ACS Nano*, 2013, **7**, 8266–8274.
- 104 X. Wang, Y. Zhang, X. Zhang, Z. Huo, X. Li, M. Que, Z. Peng, H. Wang and C. Pan, *Adv. Mater.*, 2018, **30**, e1706738.
- 105 X. Y. Wei, X. Wang, S. Y. Kuang, L. Su, H. Y. Li, Y. Wang, C. Pan, Z. L. Wang and G. Zhu, *Adv. Mater.*, 2016, **28**, 6656–6664.
- 106 M. Y. Ma, Z. Zhang, Q. L. Liao, F. Yi, L. H. Han, G. J. Zhang, S. Liu, X. Q. Liao and Y. Zhang, *Nano Energy*, 2017, **32**, 389–396.
- 107 Z. N. Zou, C. P. Zhu, Y. Li, X. F. Lei, W. Zhang and J. L. Xiao, *Sci. Adv.*, 2018, **4**, eaaq0508.
- 108 B. C. Tee, C. Wang, R. Allen and Z. Bao, *Nat. Nanotechnol.*, 2012, **7**, 825–832.
- 109 M. D. Luo, A. W. Martinez, C. Song, F. Herrault and M. G. Allen, *J. Microelectromech. Syst.*, 2014, **23**, 4–13.